

Generative Giants, Retrieval Weaklings: Why do Multimodal Large Language Models Fail at Multimodal Retrieval?

Hengyi Feng¹, Zeang Sheng², Meiyi Qiang², Wentao Zhang^{2†}

¹ University of Electronic Science and Technology of China

² Peking University

Abstract

Despite the remarkable success of multimodal large language models (MLLMs) in generative tasks, we observe that they exhibit a counterintuitive deficiency in the zero-shot multimodal retrieval task. In this work, we investigate the underlying mechanisms that hinder MLLMs from serving as effective retrievers. With the help of sparse autoencoders (SAEs), we decompose MLLM output representations into interpretable semantic concepts to probe their intrinsic behavior. Our analysis reveals that the representation space of MLLMs is overwhelmingly dominated by textual semantics; the visual information essential for multimodal retrieval only constitutes a small portion. This imbalance is compounded by the heavy focus of MLLMs on bridging image-text modalities, which facilitates generation but homogenizes embeddings and finally diminishes the discriminative power required for multimodal retrieval. We further discover that the specific feature components that contribute most to the similarity computations for MLLMs are in fact distractors that actively degrade retrieval performance. Overall, our work provides the first in-depth interpretability analysis of MLLM representations in the context of multimodal retrieval and offers possible directions for enhancing the multimodal retrieval capabilities of MLLMs.

1 Introduction

Rapid advances in multimodal large language models (MLLMs) (Xu et al., 2025; Team et al., 2025; Steiner et al., 2024; Liu et al., 2024) have revolutionized cross-modality understanding, establishing state-of-the-art performance in generative tasks such as image captioning, visual question answering (VQA), and complex visual reasoning (Caffagni et al., 2024; Bai et al., 2024). This proficiency stems largely from their massive parameter scale (Kaplan et al., 2020), which enables the capture of deep semantic dependencies (Zhang

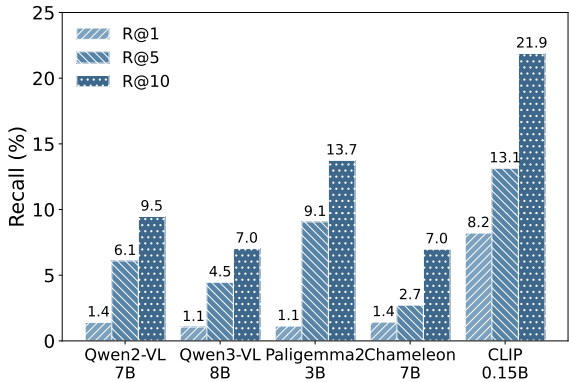


Figure 1: Multimodal retrieval performance of MLLMs and CLIP on the CIRR ($(q_i, q_t) \rightarrow c_i$) dataset. The results illustrate the inferior performance of MLLMs.

et al., 2025a) and the storage of rich parametric knowledge (Cheng et al., 2024). Consequently, there is a growing interest in exploring the potential of MLLMs for tasks extending beyond generative applications (Jiang et al., 2024b; Cai et al., 2025).

As a core task in information retrieval (IR), multimodal retrieval aims to locate relevant content across different data modalities. A dominant paradigm within this field is dense retrieval, where queries and candidates (e.g., images and texts) are mapped into a shared high-dimensional vector space. In this setting, the semantic relationship between modalities is measured by embedding similarity (Fang et al., 2024). The models responsible for encoding these inputs into vector representations are typically referred to as retrievers.

Intuitively, the extensive parametric memory and semantic understanding of MLLMs should equip them to act as capable retrievers, enabling fine-grained content encoding. However, in practice, we observe a counterintuitive phenomenon: embeddings directly derived from MLLMs yield poor performance in zero-shot multimodal retrieval task (Fig. 1). Surprisingly, MLLMs are significantly outperformed by contrastive vision-language mod-

els (e.g., CLIP (Radford et al., 2021)), although MLLMs have far more parameters than the latter. Although MLLMs are not explicitly optimized for representation learning objectives, the magnitude of this performance gap suggests a fundamental limitation when repurposing these generative giants as retrievers.

Understanding the limitations behind this failure offers key insights for expanding the use of MLLMs in the multimodal retrieval task. In this paper, we aim to answer the following research question:

What hinders MLLMs from being effective multimodal retrievers?

To address this question, we dissect the internal representational mechanisms of MLLMs. We employ sparse autoencoders (SAEs) (Huben et al., 2024) as the key analytical tool to disentangle dense representations into linear combinations of interpretable semantic concepts. Drawing inspiration from recent work (Papadimitriou et al., 2025), we introduce quantitative metrics to probe the representational space from multiple angles, explicitly linking these properties to their impact on the multimodal retrieval performance of MLLMs. Rigorous empirical experiments are conducted on a diverse set of MLLM architectures (Team, 2025; Wang et al., 2024; Team, 2024; Steiner et al., 2024), training SAEs on top of billions of activations.

Through this analysis, we identify three primary factors that limit MLLMs from being effective multimodal retrievers:

- We demonstrate that the representational spaces of MLLMs are dominated by the text modality. This inherent bias constrains the capacity to encode visual information essential for retrieval.
- We analyze how MLLMs allocate their representational budget and find a heavy concentration in bridging the modality gap. While beneficial for generation, this alignment reduces the distinctiveness of the derived embeddings.
- When MLLMs act as retrievers, the components that exert the greatest influence on similarity scores turn out to be counterproductive distractors for multimodal retrieval.

To our knowledge, our work is the first study to analyze MLLM representations and identify intrinsic factors that compromise their performance on multimodal retrieval task.

2 Preliminary: zero-shot multimodal retrieval with MLLMs

In this work, we study the multimodal retrieval task in the zero-shot setting. Given a query q , the goal is to retrieve a list of candidates $\{c_1, c_2, \dots, c_k\} \in \mathcal{C}$ that maximize ranking metrics such as Recall@1. The queries and candidates can be text, image, or mixed text–image inputs: $q \in \{q_t, q_i, (q_t, q_i)\}$; $c \in \{c_t, c_i, (c_t, c_i)\}$. We use multimodal large language models (MLLMs) to extract embeddings for both queries and candidates.

Although MLLMs can produce hidden-state representations, they are not originally designed as embedding models. Prior works (Liu et al., 2025; Lin et al., 2025) typically use the hidden state of the last token (or special tokens) as the embedding, but such representation works well only when the model has been explicitly optimized for representation learning. In the zero-shot setting considered here, where no such optimization is allowed, these embeddings are suboptimal. Instead, we observe that mean pooling over all hidden states yields consistently better performance (see Appendix C for details). In this work, unless otherwise specified, we adopt mean pooling over the hidden states of the last layer as the embedding for all MLLM-based multimodal retrieval experiments.

3 What hinders MLLMs from being effective retrievers? A mechanistic analysis with sparse autoencoders

To analyze why MLLMs underperform in zero-shot multimodal retrieval scenarios, we perform a mechanistic interpretability analysis using sparse autoencoders (SAEs) (Olshausen and Field, 1997; Makhzani and Frey, 2014).

SAEs have gained widespread popularity in recent years due to their ability to interpret language model activations (Bricken et al., 2023; Rajamoharan et al., 2024). By reconstructing internal representations with sparsely activated features, SAEs disentangle the representations into semantic concepts (Yin et al., 2025; Kissane et al., 2024; Makelov et al., 2024). Given the latent representations $H \in \mathbb{R}^{n \times d}$, the corresponding sparse codes $Z \in \mathbb{R}^{n \times c}$ are computed as:

$$Z = \Phi(HW_{enc}^\top + b), \quad \hat{H} = ZD^\top, \quad (1)$$

where $W_{enc} \in \mathbb{R}^{c \times d}$ is the learned weight matrix and $D \in \mathbb{R}^{c \times d}$ is the learned dictionary, $b \in \mathbb{R}^c$ is

the bias vector, and $\Phi(\cdot)$ denotes a nonlinear activation function such as ReLU. Specifically, each row of D can be regarded as a distinct concept vector, capturing an interpretable direction. The reconstruction loss of the SAE is then defined as:

$$\mathcal{L}_{rec}(H) = \|H - \hat{H}\|^2 + \alpha \|Z\|_1, \quad (2)$$

where the first term ensures faithful reconstruction of the input representation, and the second term enforces sparsity on the latent code through the ℓ_1 -norm, controlled by a parameter α .

In our work, we consider representative MLLMs of different architectures, including Qwen3-VL-8B-Instruct (Team, 2025), Qwen2-VL-7B-Instruct (Wang et al., 2024), Chameleon-7B (Team, 2024) and Paligemma2-3B-Mix-224 (Steiner et al., 2024). For contrastive VLMs, we consider CLIP (Clip-Vit-Base-Patch32) (Radford et al., 2021) and SigLip2 (SigLip2-Base-Patch16-512) (Tschannen et al., 2025). In our experiments, we employ Top-K SAEs (Gao et al., 2024) to learn interpretable concept representations from the activations of the COCO (Lin et al., 2014) dataset, using the last-layer hidden states for MLLMs and the last-layer embeddings extracted from contrastive VLMs. Further implementation and training details are provided in Appendix A.

3.1 Evaluation metrics of learned concepts

To evaluate and analyze the learned representations, we introduce four distinct metrics: *energy*, *modality score*, *bridge score* (Papadimitriou et al., 2025), and *retrieval attribution score*. Each measure provides unique insight by focusing on a specific dimension of the representational space.

Energy. Energy represents how frequently a concept is activated across samples. Specifically, for concept i , it is defined as the expected activation magnitude over all samples:

$$\text{Energy}_i = \mathbb{E}_z [z_i]. \quad (3)$$

Concepts with higher energy are activated more frequently or strongly, capturing more dominant or widely shared patterns in the representation space.

Modality Score. The modality score quantifies a concept’s bias toward text or image. For concept i , the modality score is computed as follows:

$$\text{ModalityScore}_i = \frac{\mathbb{E}_{z \sim \tau} [z_i]}{\mathbb{E}_{z \sim \iota} [z_i] + \mathbb{E}_{z \sim \tau} [z_i]}, \quad (4)$$

where ι and τ denote the image and text modalities, respectively. For a given concept, higher scores indicate text dominance, whereas lower scores indicate image dominance. Concepts with balanced scores act as shared cross modality features.

Bridge Score. The bridge score $\mathbf{B} \in \mathbb{R}^{c \times c}$ quantifies the extent to which a concept serves as a connector between the image and the text modalities. It is defined as:

$$\mathbf{B} = \mathbb{E}_{(z_\iota, z_\tau) \sim \gamma} [z_\iota^\top z_\tau] (z_\iota, z_\tau) \odot (D D^\top), \quad (5)$$

where $(z_\iota, z_\tau) \sim \gamma$ denotes the pair of sparse codes obtained from a matching image-text pair, and \odot denotes the Hadamard product. Higher bridge scores indicate concepts that function as semantic connectors across the two modalities.

Retrieval Attribution Score. The retrieval attribution score $\mathbf{A} \in \mathbb{R}^c$ measures the contribution of each concept to the overall cross modality similarity between image and text representations. The contribution of each concept is decomposed through reconstruction interactions:

$$\mathbf{A} = \mathbb{E}_{(z_\iota, z_\tau) \sim \gamma} [z_\iota \odot (M z_\tau) + z_\tau \odot (M z_\iota)], \quad (6)$$

where $M = D^\top D$. The score is tailored for multimodal retrieval settings and measures each concept’s impact on cross modality matching, with higher scores indicating greater influence on the final similarity between queries and candidates.

3.2 Observation: Textual information dominates representations in MLLMs

Key Takeaway

The strong text bias in MLLMs’ representational space limits the encoding of visual information and undermines multimodal retrieval effectiveness.

We first analyze the distribution of the *modality score* (Eq. 4). In all models that we analyze, as shown in Figure 2, our first observation is that the majority of the learned concepts are single-modality. Meanwhile, the concepts learned by MLLMs exhibit a strong bias towards the text modality. The distribution of modality scores reveals that a large proportion of concepts are text-specific, indicating that the MLLM-generated representations are primarily driven by linguistic information rather than visual information.

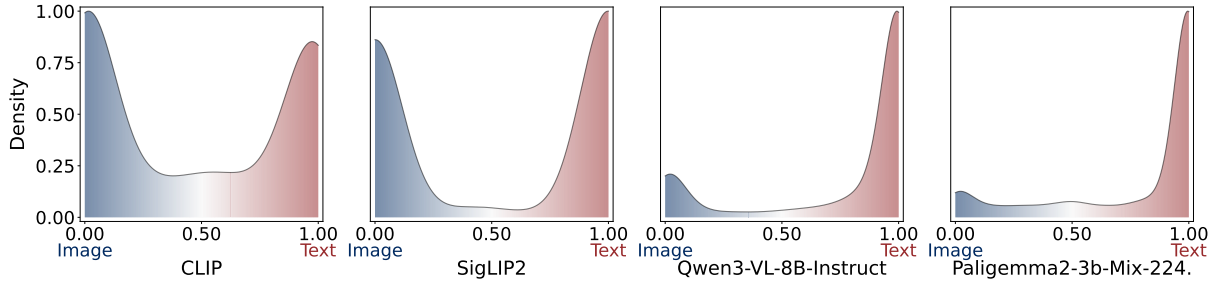


Figure 2: Distribution of *modality scores* for learned concepts by (a) CLIP, (b) SigLIP2, (c) Qwen3-VL-8B-Instruct, and (d) Paligemma2-3b-Mix-224. The Modality Score quantifies the bias of each concept towards the image modality (blue region) or the text modality (red region). The distributions are visualized using Kernel Density Estimation (Parzen, 1962) based on concept activation statistics.

However, unlike MLLMs, the distribution of image- and text-specific concepts is more balanced in CLIP and SigLIP2. Moreover, they exhibit a larger fraction of intermediate concepts, which encode information from both modalities, serving as shared semantic anchors that better align visual and textual representations.

Previous studies have discussed the existence of modality bias (Zheng et al., 2025) and modality gap (Liang et al., 2022; Eslami and de Melo, 2025) in multimodal models. In the context of multimodal retrieval, we argue that maintaining a balanced modality representation is particularly important. When a model’s representations are heavily biased toward one modality, its embeddings fail to adequately represent samples from the other, leading to degraded retrieval performance under cross-modality or mix-modality retrieval scenarios. In contrast, contrastive VLMs, with more balanced and interconnected concept spaces, are more capable of producing modality-agnostic embeddings, achieving better performance in zero-shot multimodal retrieval settings than MLLMs.

3.3 Observation: MLLMs concentrate most of their representational efforts on bridging image-text modalities

Key Takeaway

MLLMs overly align visual information into the text space, producing embeddings that are less distinctive across samples and impairing multimodal retrieval performance.

When we examine the *energy* (Eq. 3) distribution of the learned concepts, it is observed that for all models, the distribution exhibits a pronounced long-tail pattern (Fig. 3). This reveals that during

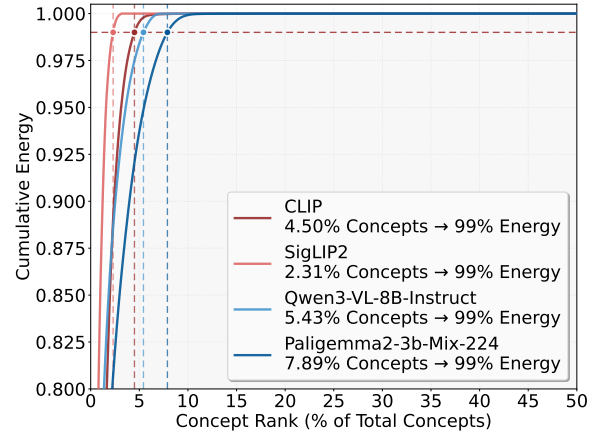


Figure 3: Cumulative *energy* distribution across concept ranks for different multimodal models. The curves show the percentage of total energy captured as concepts are ranked by their individual energy values.

the reconstruction process, only a small subset of concepts is repeatedly activated across different samples. These concepts constitute the main concentrations of the model’s representational space. We suggest that they play a critical role in shaping the overall embedding structure.

To further explore where this representational energy is allocated, we analyze two additional metrics, *bridge score* (Eq. 5) and *retrieval attribution score* (Eq. 6), for a joint analysis. Our goal is to uncover how multimodal models, particularly MLLMs, distribute their energy across concepts and how such allocation patterns affect their retrieval performance. Specifically, for each concept, we compute its energy, bridge score, and retrieval attribution score, and then extract the top 1% concepts for each metric. We measure the Jaccard similarity between these top sets to quantify the degree of overlap, where a higher overlap demonstrates that the same set of concepts dominates multiple

Table 1: Jaccard similarity between top 1% concept sets across three different evaluation metrics. \mathcal{S}_E : top *energy* set, \mathcal{S}_A : top *retrieval attribution score* set, \mathcal{S}_B : top *bridge score* set.

Type	Model	$J(\mathcal{S}_E, \mathcal{S}_A)$	$J(\mathcal{S}_E, \mathcal{S}_B)$	$J(\mathcal{S}_A, \mathcal{S}_B)$	Triple Overlap
Contrastive VLMs	CLIP	0.5674	0.6831	0.6126	0.4796
	SigLIP2	0.3948	0.5775	0.3783	0.2915
MLLMs	Qwen2-VL-7B-Instruct	0.6494	0.7957	0.7146	0.5989
	Qwen3-VL-8B-Instruct	0.6610	0.8547	0.6700	0.5486
	Paligemma2-3B-Mix-224	0.7655	0.8085	0.7124	0.6541
	Chameleon-7B	0.6850	0.8591	0.7099	0.5953

representational dimensions.

Formally, for two concept sets \mathcal{A} and \mathcal{B} , the Jaccard similarity is computed as:

$$J(\mathcal{A}, \mathcal{B}) = \frac{|\mathcal{A} \cap \mathcal{B}|}{|\mathcal{A} \cup \mathcal{B}|}. \quad (7)$$

As shown in Table 1, both MLLMs and contrastive VLMs exhibit significant overlaps between the concepts of high-energy, high-bridge, and high-retrieval attribution score sets. However, the overlap ratios are consistently higher in MLLMs. Notably, the intersection between high-energy and high-bridge score concepts is particularly strong. This suggests that MLLMs devote a large portion of their representational energy to bridging modalities, attempting to harmonize image and text representations within a unified latent space.

At first glance, this behavior might appear beneficial for multimodal integration and even for retrieval. However, when combined with the findings discussed in Section 3.2, a clearer picture emerges: MLLMs primarily align multimodal information by projecting visual information towards the text space, rather than establishing a balanced semantic fusion. This could lead to an inferior ability of MLLMs to encode visual information.

To validate this, we conduct an additional experiment. Before mean pooling, we mask out the hidden states corresponding to image tokens and then recompute the final embeddings. As shown in Figure 4, we find that removing image tokens results in only marginal changes in retrieval performance, while masking the user prompt region lead to a sharp performance decline.

From a retrieval task perspective, effective retrieval performance largely depends on the distinctiveness of embeddings between samples. When we examined the overlap between high-retrieval attribution score concepts (those most relevant to retrieval) and the high-energy / high-bridge score concepts, we observe a significant intersection among

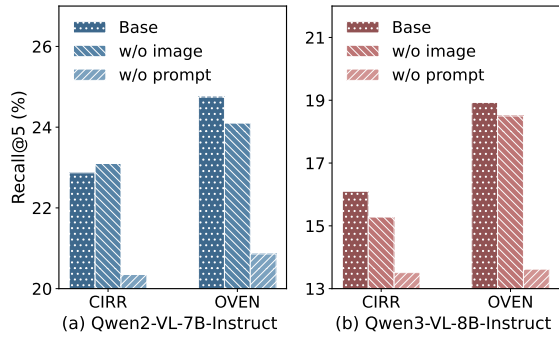


Figure 4: Retrieval performance on the subset (3k queries) of CIRR ($(q_i, q_t) \rightarrow c_i$) and OVEN ($(q_i, q_t) \rightarrow (c_i, c_t)$) datasets. “Base” uses the full input; “w/o image” and “w/o prompt.” denote the removal of image tokens and prompt tokens, respectively.

concepts learned from MLLMs. This suggests that the same dominant concepts not only consume most of the representational energy but also contribute most to multimodal similarity estimation. Consequently, the embeddings of different samples become concentrated around similar text-driven features with limited discriminability.

Meanwhile, contrastive VLMs display weaker overlap among these metrics. The high-energy, high-bridge score, and high-retrieval attribution score concepts are more loosely coupled, allowing them to provide representations with greater discriminability. This ultimately contributes to their superior retrieval performance in multimodal retrieval.

3.4 Observation: Dominant components in similarity computations are counterproductive for retrieval

Key Takeaway

When MLLMs act as retrievers, the components exerting the greatest influence on similarity scores are in fact counterproductive distractors for multimodal retrieval.

Table 2: Retrieval performance on a 3k-query subset of COCO ($q_i \rightarrow c_t$) before (Base) and after removing the subspace spanned by concepts with high retrieval attribution scores (Removal), evaluated on Qwen2-VL-7B (**Qwen2-VL-7B-Instruct**), Qwen3-VL-8B (**Qwen3-VL-8B-Instruct**), PaliGemma2-3B (**Paligemma2-3B-Mix-224**), and **Chameleon-7B**.

Model	Setting	R@1	R@5	R@10
Qwen2-VL-7B	Base	2.95	9.53	15.13
	Removal	7.18	20.91	31.18
Qwen3-VL-8B	Base	2.60	7.88	12.33
	Removal	4.23	13.53	20.72
PaliGemma2-3B	Base	6.07	15.46	21.55
	Removal	24.47	48.79	61.03
Chameleon-7B	Base	1.79	7.58	10.12
	Removal	3.32	14.29	16.87

A core objective of multimodal retrieval is to compute a reliable similarity metric between query and candidate embeddings. Given the suboptimal performance of MLLMs in retrieval tasks, a critical question arises: *Do the representational components that exert the greatest influence on the final similarity calculation genuinely contribute to retrieval performance?*

To investigate this, we propose an ablation strategy that removes the components corresponding to concepts that exhibit high **retrieval attribution scores** (Eq.6) from the representational space.

Concretely, let $D_R \subseteq D$ denote the sub-dictionary formed by the concept atoms whose retrieval attribution scores fall in the top 1% (m concepts). To characterize the subspace \mathcal{S} spanned by these concepts with high influence, we perform Singular Value Decomposition (SVD) on D_R :

$$D_R = U\Sigma V^\top, \quad (8)$$

where $V \in \mathbb{R}^{d \times m}$ contains the right singular vectors that form an orthonormal basis for directions in the embedding space. We select the top r right singular vectors $V_r \in \mathbb{R}^{d \times r}$ to construct the basis for the subspace \mathcal{S} .

Given the embedding $h \in \mathbb{R}^d$, we project it onto \mathcal{S} to isolate the components associated with D_R :

$$\Pi_{\mathcal{S}}(h) = V_r V_r^\top h. \quad (9)$$

We then compute the representation with the effect of D_R removed by subtracting this projection:

$$\tilde{h} = h - \Pi_{\mathcal{S}}(h). \quad (10)$$

The resulting residual embedding \tilde{h} is normalized and utilized directly for retrieval.

The retrieval performance using the transformed embeddings is reported in Table 2, and the results reveal that removing the concepts with the highest retrieval attribution scores yields a significant improvement in retrieval accuracy.

This suggests that the components dominating the similarity calculation in MLLM-derived embeddings are, in effect, counterproductive for retrieval tasks. While these concepts possess heavy influence on the dot product magnitude, they appear to act as "distractors" that inflate similarity scores regardless of semantic relevance. This implies that in the raw representational spaces of MLLMs, the semantically discriminative features necessary for precise retrieval are severely overshadowed.

4 Related works

4.1 Multimodal large language models

Multimodal large language models (MLLMs) have achieved remarkable success in a wide range of tasks (Caffagni et al., 2024; Zhou et al., 2024). Prominent MLLMs such as LLaVA (Liu et al., 2023a, 2024), Qwen-VL (Team, 2025), Paligemma2 (Steiner et al., 2024), InternVL (Wang et al., 2025) and MiniCPM-V (Yao et al., 2024) have shown promising advances in generative tasks such as image captioning, visual question answering, and complex visual reasoning (Sarto et al., 2025; Sun et al., 2025; Liang et al., 2024).

4.2 Multimodal retrieval

Multimodal retrieval aims to align diverse modalities (e.g., text, images, or mixed text–image) within a shared embedding space for semantic similarity matching. Early multimodal retrieval approaches largely utilize pre-trained models such as CLIP (Radford et al., 2021) or BLIP (Li et al., 2022) for multimodal embedding. For instance, UniVL-DR (Liu et al., 2023b) and UniR (Wei et al., 2024) encode images and texts using CLIP or BLIP encoders separately, followed by fusion strategies.

With the advancement of MLLMs, researchers have begun to explore the potential of leveraging MLLMs in multimodal retrieval tasks (Liu et al., 2025; Lan et al., 2025; Kong et al., 2025). Specifically, a line of work focuses on building embedding models based on pretrained MLLMs to enhance multimodal retrieval, such as E5-V (Jiang et al., 2024a), VLM2Vec (Jiang et al., 2024b), MM-

Embed (Lin et al., 2025), and CAFE (Yu et al., 2025). However, these methods typically require substantial computational resources and often rely on multi-stage training strategies (Zhang et al., 2025b), which introduce additional costs. In this paper, we are the first to systematically analyze the representational spaces of MLLMs from a multimodal retrieval perspective. Based on our observations, we propose a training-free approach that leverages intrinsic properties of MLLM embeddings to improve retrieval performance without the need for additional model training.

5 Conclusion

In this work, we investigate why multimodal large language models (MLLMs), despite their strong generative prowess, fail to function as effective zero-shot multimodal retrievers. By leveraging sparse autoencoders (SAEs) to decompose their internal representations, we reveal that MLLMs operate in a representational space overwhelmingly dominated by textual semantics, which suppresses essential visual information. Furthermore, we find that the emphasis on bridging modalities for generation leads to homogenized embeddings, reducing the discriminative power required for retrieval, while the features most influential to similarity scores paradoxically act as distractors. Together, these findings provide the first in-depth interpretability analysis of MLLMs in the retrieval context, offering insights for designing future MLLM-based retriever architectures.

References

Tianyi Bai, Hao Liang, Binwang Wan, Yanran Xu, Xi Li, Shiyu Li, Ling Yang, Bozhou Li, Yifan Wang, Bin Cui, and 1 others. 2024. A survey of multimodal large language model from a data-centric perspective. *arXiv preprint arXiv:2405.16640*.

Trenton Bricken, Adly Templeton, Joshua Batson, Brian Chen, Adam Jermyn, Tom Conerly, Nick Turner, Cem Anil, Carson Denison, Amanda Askell, and 1 others. 2023. Towards monosemanticity: Decomposing language models with dictionary learning. *Transformer Circuits Thread*, 2.

Davide Caffagni, Federico Cocchi, Luca Barsellotti, Nicholas Moratelli, Sara Sarto, Lorenzo Baraldi, Marcella Cornia, and Rita Cucchiara. 2024. The revolution of multimodal large language models: A survey. In *Annual Meeting of the Association for Computational Linguistics*.

Qifeng Cai, Hao Liang, Hejun Dong, Meiyi Qiang, Ruichuan An, Zhaoyang Han, Zhengzhou Zhu, Bin Cui, and Wentao Zhang. 2025. Lovr: A benchmark for long video retrieval in multimodal contexts. *arXiv preprint arXiv:2505.13928*.

Sitao Cheng, Liangming Pan, Xunjian Yin, Xinyi Wang, and William Yang Wang. 2024. Understanding the interplay between parametric and contextual knowledge for large language models. *Preprint*, arXiv:2410.08414.

Sedigheh Eslami and Gerard de Melo. 2025. Mitigate the gap: Improving cross-modal alignment in CLIP. In *The Thirteenth International Conference on Learning Representations*.

Yan Fang, Jingtao Zhan, Qingyao Ai, Jiaxin Mao, Weihang Su, Jia Chen, and Yiqun Liu. 2024. Scaling laws for dense retrieval. In *Proceedings of the 47th International ACM SIGIR Conference on Research and Development in Information Retrieval, SIGIR '24*, page 1339–1349, New York, NY, USA. Association for Computing Machinery.

Stephanie Fu, Netanel Tamir, Shobhita Sundaram, Lucy Chai, Richard Zhang, Tali Dekel, and Phillip Isola. 2023. Dreamsim: Learning new dimensions of human visual similarity using synthetic data. *arXiv preprint arXiv:2306.09344*.

Leo Gao, Tom Dupr'e la Tour, Henk Tillman, Gabriel Goh, Rajan Troll, Alec Radford, Ilya Sutskever, Jan Leike, and Jeffrey Wu. 2024. Scaling and evaluating sparse autoencoders. *ArXiv*, abs/2406.04093.

Robert Huben, Hoagy Cunningham, Logan Riggs Smith, Aidan Ewart, and Lee Sharkey. 2024. Sparse autoencoders find highly interpretable features in language models. In *The Twelfth International Conference on Learning Representations, ICLR 2024, Vienna, Austria, May 7-11, 2024*. OpenReview.net.

Ting Jiang, Minghui Song, Zihan Zhang, Haizhen Huang, Weiwei Deng, Feng Sun, Qi Zhang, Deqing Wang, and Fuzhen Zhuang. 2024a. E5-v: Universal embeddings with multimodal large language models. *ArXiv*, abs/2407.12580.

Ziyan Jiang, Rui Meng, Xinyi Yang, Semih Yavuz, Yingbo Zhou, and Wenhui Chen. 2024b. Vlm2vec: Training vision-language models for massive multimodal embedding tasks. *ArXiv*, abs/2410.05160.

Jared Kaplan, Sam McCandlish, Tom Henighan, Tom B. Brown, Benjamin Chess, Rewon Child, Scott Gray, Alec Radford, Jeffrey Wu, and Dario Amodei. 2020. Scaling laws for neural language models. *Preprint*, arXiv:2001.08361.

Connor Kissane, Robert Krzyzanowski, Joseph Isaac Bloom, Arthur Conmy, and Neel Nanda. 2024. Interpreting attention layer outputs with sparse autoencoders. *arXiv preprint arXiv:2406.17759*.

Fanheng Kong, Jingyuan Zhang, Yahui Liu, Hongzhi Zhang, Shi Feng, Xiaocui Yang, Daling Wang, Yu Tian, Victoria W., Fuzheng Zhang, and Guorui Zhou. 2025. Modality curation: Building universal embeddings for advanced multimodal information retrieval. *arXiv preprint arXiv:2505.19650*.

Zhibin Lan, Liqiang Niu, Fandong Meng, Jie Zhou, and Jinsong Su. 2025. **LLaVE: Large language and vision embedding models with hardness-weighted contrastive learning**. In *Findings of the Association for Computational Linguistics: EMNLP 2025*, pages 13721–13735, Suzhou, China. Association for Computational Linguistics.

Junnan Li, Dongxu Li, Caiming Xiong, and Steven C. H. Hoi. 2022. **Blip: Bootstrapping language-image pre-training for unified vision-language understanding and generation**. In *International Conference on Machine Learning*.

Hao Liang, Zirong Chen, and Wentao Zhang. 2024. **Evqascore: Efficient video question answering data evaluation**. *arXiv preprint arXiv:2411.06908*.

Weixin Liang, Yuhui Zhang, Yongchan Kwon, Serena Yeung, and James Zou. 2022. Mind the gap: understanding the modality gap in multi-modal contrastive representation learning. In *Proceedings of the 36th International Conference on Neural Information Processing Systems, NIPS '22*, Red Hook, NY, USA. Curran Associates Inc.

Sheng-Chieh Lin, Chankyu Lee, Mohammad Shoeybi, Jimmy Lin, Bryan Catanzaro, and Wei Ping. 2025. **Mm-embed: Universal multimodal retrieval with multimodal LLMS**. In *The Thirteenth International Conference on Learning Representations, ICLR 2025, Singapore, April 24-28, 2025*. OpenReview.net.

Tsung-Yi Lin, Michael Maire, Serge J. Belongie, James Hays, Pietro Perona, Deva Ramanan, Piotr Dollár, and C. Lawrence Zitnick. 2014. **Microsoft COCO: common objects in context**. In *Computer Vision - ECCV 2014 - 13th European Conference, Zurich, Switzerland, September 6-12, 2014, Proceedings, Part V*, volume 8693 of *Lecture Notes in Computer Science*, pages 740–755. Springer.

Haotian Liu, Chunyuan Li, Yuheng Li, and Yong Jae Lee. 2023a. **Improved baselines with visual instruction tuning**. *Preprint*, arXiv:2310.03744.

Haotian Liu, Chunyuan Li, Yuheng Li, Bo Li, Yuanhan Zhang, Sheng Shen, and Yong Jae Lee. 2024. **Llava-next: Improved reasoning, ocr, and world knowledge**.

Yikun Liu, Yajie Zhang, Jiayin Cai, Xiaolong Jiang, Yao Hu, Jiangchao Yao, Yanfeng Wang, and Weidi Xie. 2025. **Lamra: Large multimodal model as your advanced retrieval assistant**. In *IEEE/CVF Conference on Computer Vision and Pattern Recognition, CVPR 2025, Nashville, TN, USA, June 11-15, 2025*, pages 4015–4025. Computer Vision Foundation / IEEE.

Zhenghao Liu, Chenyan Xiong, Yuanhuiyi Lv, Zhiyuan Liu, and Ge Yu. 2023b. Universal vision-language dense retrieval: Learning a unified representation space for multi-modal retrieval. In *Proceedings of ICLR*.

Aleksandar Makelov, George Lange, and Neel Nanda. 2024. Towards principled evaluations of sparse autoencoders for interpretability and control. *arXiv preprint arXiv:2405.08366*.

Alireza Makhzani and Brendan Frey. 2014. **k-sparse autoencoders**. *Preprint*, arXiv:1312.5663.

Neel Nanda. 2023. **Open Source Replication & Commentary on Anthropic’s Dictionary Learning Paper**.

Bruno A. Olshausen and David J. Field. 1997. **Sparse coding with an overcomplete basis set: A strategy employed by v1?** *Vision Research*, 37:3311–3325.

Isabel Papadimitriou, Huangyuan Su, Thomas Fel, Naomi Saphra, Sham M. Kakade, and Stephanie Gil. 2025. **Interpreting the linear structure of vision-language model embedding spaces**. *CoRR*, abs/2504.11695.

Emanuel Parzen. 1962. **On estimation of a probability density function and mode**. *Annals of Mathematical Statistics*, 33:1065–1076.

Alec Radford, Jong Wook Kim, Chris Hallacy, Aditya Ramesh, Gabriel Goh, Sandhini Agarwal, Girish Sastry, Amanda Askell, Pamela Mishkin, Jack Clark, Gretchen Krueger, and Ilya Sutskever. 2021. **Learning transferable visual models from natural language supervision**. *Preprint*, arXiv:2103.00020.

Senthoothan Rajamanoharan, Tom Lieberum, Nicolas Sonnerat, Arthur Conmy, Vikrant Varma, János Kramár, and Neel Nanda. 2024. Jumping ahead: Improving reconstruction fidelity with jumprelu sparse autoencoders. *arXiv preprint arXiv:2407.14435*.

Sara Sarto, Marcella Cornia, and Rita Cucchiara. 2025. **Image captioning evaluation in the age of multimodal llms: Challenges and future perspectives**. *Preprint*, arXiv:2503.14604.

Andreas Steiner, André Susano Pinto, Michael Tschannen, Daniel Keysers, Xiao Wang, Yonatan Bitton, Alexey Gritsenko, Matthias Minderer, Anthony Sherbony, Shangbang Long, Siyang Qin, Reeve Ingle, Emanuele Bugliarello, Sahar Kazemzadeh, Thomas Mesnard, Ibrahim Alabdulmohsin, Lucas Beyer, and Xiaohua Zhai. 2024. **Paligemma 2: A family of versatile vlms for transfer**. *Preprint*, arXiv:2412.03555.

Linzhuang Sun, Hao Liang, Jingxuan Wei, Bihui Yu, Tianpeng Li, Fan Yang, Zenan Zhou, and Wentao Zhang. 2025. **Mm-verify: Enhancing multimodal reasoning with chain-of-thought verification**. *arXiv preprint arXiv:2502.13383*.

Chameleon Team. 2024. **Chameleon: Mixed-modal early-fusion foundation models**. *arXiv preprint arXiv:2405.09818*.

Gemma Team, Aishwarya Kamath, Johan Ferret, Shreya Pathak, Nino Vieillard, Ramona Merhej, Sarah Perrin, Tatiana Matejovicova, Alexandre Ramé, Morgane Rivière, Louis Rouillard, Thomas Mesnard, Geoffrey Cideron, Jean bastien Grill, Sabela Ramos, Edouard Yvinec, Michelle Casbon, Etienne Pot, Ivo Penchev, and 197 others. 2025. [Gemma 3 technical report](#). *Preprint*, arXiv:2503.19786.

Qwen Team. 2025. [Qwen3 technical report](#). *Preprint*, arXiv:2505.09388.

Michael Tschannen, Alexey Gritsenko, Xiao Wang, Muhammad Ferjad Naeem, Ibrahim Alabdulmohsin, Nikhil Parthasarathy, Talfan Evans, Lucas Beyer, Ye Xia, Basil Mustafa, Olivier Hénaff, Jeremiah Harmsen, Andreas Steiner, and Xiaohua Zhai. 2025. [Siglip 2: Multilingual vision-language encoders with improved semantic understanding, localization, and dense features](#). *Preprint*, arXiv:2502.14786.

Peng Wang, Shuai Bai, Sinan Tan, Shijie Wang, Zhihao Fan, Jinze Bai, Keqin Chen, Xuejing Liu, Jialin Wang, Wenbin Ge, Yang Fan, Kai Dang, Mengfei Du, Xuancheng Ren, Rui Men, Dayiheng Liu, Chang Zhou, Jingren Zhou, and Junyang Lin. 2024. [Qwen2-vl: Enhancing vision-language model’s perception of the world at any resolution](#). *Preprint*, arXiv:2409.12191.

Weiyun Wang, Zhangwei Gao, Lixin Gu, Hengjun Pu, Long Cui, Xinguang Wei, Zhaoyang Liu, Linglin Jing, Shenglong Ye, Jie Shao, and 1 others. 2025. [Internvl3.5: Advancing open-source multimodal models in versatility, reasoning, and efficiency](#). *arXiv preprint arXiv:2508.18265*.

Cong Wei, Yang Chen, Haonan Chen, Hexiang Hu, Ge Zhang, Jie Fu, Alan Ritter, and Wenhui Chen. 2024. [Uniir: Training and benchmarking universal multimodal information retrievers](#). In *Computer Vision – ECCV 2024: 18th European Conference, Milan, Italy, September 29–October 4, 2024, Proceedings, Part LXXXVII*, page 387–404, Berlin, Heidelberg. Springer-Verlag.

Jin Xu, Zhifang Guo, Hangrui Hu, Yunfei Chu, Xiong Wang, Jinzheng He, Yuxuan Wang, Xian Shi, Ting He, Xinfu Zhu, Yuanjun Lv, Yongqi Wang, Dake Guo, He Wang, Linhan Ma, Pei Zhang, Xinyu Zhang, Hongkun Hao, Zishan Guo, and 19 others. 2025. [Qwen3-omni technical report](#). *Preprint*, arXiv:2509.17765.

Yuan Yao, Tianyu Yu, Ao Zhang, Chongyi Wang, Junbo Cui, Hongji Zhu, Tianchi Cai, Haoyu Li, Weilin Zhao, Zihui He, and 1 others. 2024. [Minicpm-v: A gpt-4v level mllm on your phone](#). *arXiv preprint arXiv:2408.01800*.

Qingyu Yin, Chak Tou Leong, Minjun Zhu, Hanqi Yan, Qiang Zhang, Yulan He, Wenjie Li, Jun Wang, Yue Zhang, and Linyi Yang. 2025. [Constrain alignment with sparse autoencoders](#). *Preprint*, arXiv:2411.07618.

Hao Yu, Zhuokai Zhao, Shen Yan, Lukasz Korycki, Jianyu Wang, Baosheng He, Jiayi Liu, Lizhu Zhang, Xiangjun Fan, and Hanchao Yu. 2025. [Cafe: Unifying representation and generation with contrastive-autoregressive finetuning](#). *ArXiv*, abs/2503.19900.

Jiarui Zhang, Mahyar Khayatkhoei, Prateek Chhikara, and Filip Ilievski. 2025a. [Mllms know where to look: Training-free perception of small visual details with multimodal llms](#). In *The Thirteenth International Conference on Learning Representations, ICLR 2025, Singapore, April 24–28, 2025*. OpenReview.net.

Xin Zhang, Yanzhao Zhang, Wen Xie, Mingxin Li, Ziqi Dai, Dingkun Long, Pengjun Xie, Meishan Zhang, Wenjie Li, and Min Zhang. 2025b. [Bridging modalities: Improving universal multimodal retrieval by multimodal large language models](#). *2025 IEEE/CVF Conference on Computer Vision and Pattern Recognition (CVPR)*, pages 9274–9285.

Xu Zheng, Chenfei Liao, Yuqian Fu, Kaiyu Lei, Yuanhuiyu Lyu, Lutao Jiang, Bin Ren, Jialei Chen, Jiawen Wang, Chengxin Li, Linfeng Zhang, Danda Pani Paudel, Xuanjing Huang, Yu-Gang Jiang, Nicu Sebe, Dacheng Tao, Luc Van Gool, and Xuming Hu. 2025. [Mllms are deeply affected by modality bias](#). *Preprint*, arXiv:2505.18657.

Minxuan Zhou, Hao Liang, Tianpeng Li, Zhiyu Wu, Mingan Lin, Linzhuang Sun, Yaqi Zhou, Yan Zhang, Xiaoqin Huang, Yicong Chen, and 1 others. 2024. [Mathscape: Evaluating mllms in multimodal math scenarios through a hierarchical benchmark](#). *arXiv preprint arXiv:2408.07543*.

A Training details for SAEs

In this section, we provide the comprehensive training configuration used for the sparse autoencoders (SAEs) discussed in this paper.

In our experiments, we employ Top-K SAEs (Gao et al., 2024) to learn interpretable concept representations from the activations of COCO (Lin et al., 2014) dataset ¹. The training process involves processing billions of activations; for instance, the training run for Qwen2-VL-7B-Instruct encompasses approximately 28 billion activations.

For MLLMs, we train SAEs on Qwen2-VL-7B-Instruct (Wang et al., 2024), Qwen3-VL-7B-Instruct (Team, 2025), Paligemma2-3B (Steiner et al., 2024) and Chameleon-7B (Team, 2024). For these architectures, SAEs are trained on the hidden states of the layer. These SAEs differ in input dimension, but share a fixed dictionary width of 32768. For contrastive VLMs, We utilize

¹<https://huggingface.co/datasets/lmms-lab/COCO-Caption>

CLIP (ViT-Base-Patch32) (Radford et al., 2021) and SigLip2(SigLip2-Base-Patch16-512) (Tschannen et al., 2025). The SAEs for these models are trained on the derived embeddings with a dictionary width of 7168.

We train SAEs using the Adam optimizer with $\beta_1 = 0.9$, $\beta_2 = 0.999$, and $\epsilon = 10^{-8}$. The learning rate is set to $8e-4$ for all SAEs with a batch size of 4096. Our implementation utilizes the Overcomplete² framework.

To mitigate the prohibitive RAM and VRAM costs associated with storing pre-computed embeddings for the entire dataset, we adopt a dynamic encoding strategy. Instead of pre-calculating all activations, the models encode a small proportion of the dataset on-the-fly, loading batches sequentially into GPU memory to derive the necessary activations. To ensure training stability and prevent the optimization process from learning temporal correlations present in sequential data, we maintain a shuffled buffer of these activations, following (Nanda, 2023). The SAEs sample training batches from this randomized buffer rather than directly from the sequential stream.

B Details of evaluating learned concepts

In Section 3, we employ sparse autoencoders (SAEs) to conduct a mechanistic analysis of MLLM performance in multimodal retrieval. For MLLMs, SAEs are trained on the hidden states of the final layer, which operate at the token granularity. This allows the SAEs to fully capture the representational space of the MLLM at the token level. However, for the purpose of analyzing the retrieval mechanism, our evaluation is conducted at the sample level, where each sample consists of a sequence of tokens. Here, we apply mean pooling, which is also the strategy we utilize during retrieval, to the token embeddings of each sample, aggregating them into a single embedding vector before feeding it into the SAE for analysis.

Let $h_t \in \mathbb{R}^d$ denote the t -th row of H , representing the t -th token in a sequence of length n . The representation utilized for retrieval is given by $\bar{h} = \frac{1}{n} \sum_{t=1}^n h_t$. The sparse code $z \in \mathbb{R}^c$ for the

aggregated embedding is computed as:

$$z = \Phi(\bar{h}W_{enc}^\top + b) \quad (11)$$

$$= \Phi\left(\left(\frac{1}{L} \sum_{t=1}^L h_t\right)W_{enc}^\top + b\right) \quad (12)$$

$$= \Phi\left(\frac{1}{L} \sum_{t=1}^L (h_t W_{enc}^\top) + b\right). \quad (13)$$

This demonstrates that the sparse codes of the pooled embedding is mathematically equivalent to the arithmetic mean of the sparse codes of the token level.

C Comparison of embedding extraction strategy for MLLMs

In this section, we explore strategies for extracting embeddings using MLLMs. We primarily focus on two strategies: (1) **Last token**: This method is widely adopted in the existing literature (). In this scenario, the multimodal input is typically constructed as "*<image> <text> Summarize the above image and sentence in one word: <emb>*", where "*<image>*" and "*<text>*" serve as placeholders. The hidden representation of the final token, denoted as "*<emb>*", is extracted as the embedding. While this strategy has proven effective when MLLMs are explicitly optimized for representation learning goals, it may be suboptimal for zero-shot multimodal retrieval. (2) **Mean pooling**: This strategy applies mean pooling to the representations derived from the last layer's hidden states to obtain a comprehensive embedding for the entire sequence.

To evaluate these methods, we conduct comparative experiments on zero-shot multimodal retrieval. As shown in Table 3, the mean pooling strategy consistently outperforms the last token strategy, which demonstrates significantly inferior results. Based on these findings, we adopt mean pooling over the last layer's hidden states as the default embedding extraction method for all MLLM-based retrieval experiments in this work, unless otherwise specified.

²<https://github.com/KempnerInstitute/overcomplete>

Table 3: Zero-shot multimodal retrieval performance comparison between two embedding extraction strategies: **last token** and **mean pooling** on the MSCOCO ($(q_i \rightarrow c_t)$), NIGHTS ($q_i \rightarrow c_t$), NIGHTS (Fu et al., 2023) and CIRR ($(q_i, q_t) \rightarrow c_i$) datasets.

Model	Setting	MSCOCO			NIGHTS			CIRR		
		R@1	R@5	R@10	R@1	R@5	R@10	R@1	R@5	R@10
Qwen2-VL-7B-Instruct	Last token	0.20	2.65	3.81	1.89	3.64	5.88	0.54	1.49	3.23
	Mean pooling	2.71	8.48	13.22	7.55	22.80	39.11	1.41	6.09	9.47
Qwen3-VL-8B-Instruct	Last token	0.34	2.49	3.86	1.05	2.96	5.75	0.49	1.35	3.38
	Mean pooling	2.76	7.36	11.28	6.46	20.14	36.42	1.01	4.46	17.03
Paligemma2-3B-Mix-224	Last token	1.63	3.23	5.81	1.29	4.26	8.42	0.43	1.84	4.16
	Mean pooling	5.94	14.22	19.25	8.96	24.67	44.79	1.13	9.06	13.74